**SUPPLEMENTARY MATERIAL FOR "NEOGENE SEDIMENTARY DEFORMATION IN THE CHILEAN FOREARC AND IMPLICATIONS FOR ANDEAN BASIN DEVELOPMENT, SEISMICITY AND UPLIFT"**
**by Houston, J., Hart, D. & Houston, A.**

## Petrogenesis of crackle breccia at Puente Posada

The crackle breccia at Puente Posada (see figure below) shows a relict intraclast limestone (lst) with minor fenestral porosity (F) and minor reworked volcanic ash (L). The fenestrae show some infilling with opaque calcite cement. Syneresis cracks are also resent in the limestone and are generally infilled with calcite. More than one phase of syneresis may be observed where some cracks crosscut others. The limestone is brecciated with limited block rotation, in places rupturing the calcite filled fenestrae. Interblock areas amount to as much as 30%. The interblock spaces show a three-stage vein infill. The first stage (V1) is represented by opaque calcite coating the blocks, typically 1 mm thick, and with localised microbrecciation. The second stage (V2) is a multilayered isopachous cavity infill of ferroan calcite, inclusion-rich, and having a radial fabric and crystalline botryoidal surfaces. The final stage (V3) shows partial-total infilling of remaining cavities with opaque white calcite with dark organic (?algal) inclusions.

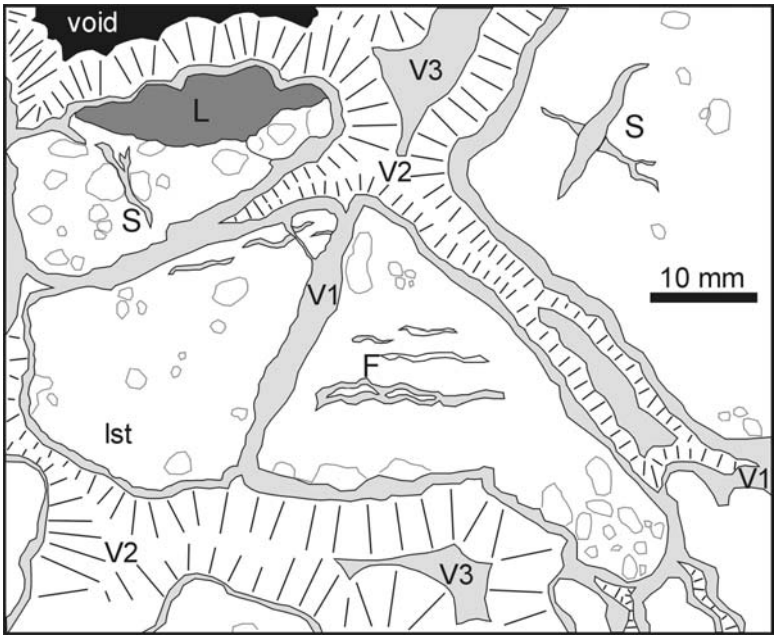


This indicates a complex polyphase diagenesis with varying applied stress and groundwater conditions. Initial limestone deposition with <5% fenestral porosity was followed by syneresis cracking adding a further ~5% porosity, possibly as a result of flooding by fresh water. Immediately after, early calcite precipitation occurred in the cracks and fenestrae, presumably under phreatic conditions. The subsequent brecciation is interpreted to be contemporaneous with the subaqueous-subaerial slumping and sliding of material at, or close to its plastic limit, of extensive occurrence in this horizon at Puente Posada. This was followed by a three-stage calcite vein infill that progressively reduced the cavity porosity formed during brecciation. It is not clear whether V1 occurred under vadose or phreatic conditions.

V2 may represent phreatic, reducing conditions, possibly due to the oxidation of organic matter upstream in the Calama Basin. The final infill (V3) may suggest late-stage vadose conditions.

**Slope stability analysis**

The stability of some typical slope configurations was investigated using the modified Bishop analysis (Bishop 1955). The configurations are shown in the figures below, where topography and layers are indicated as black lines and the alternative phreatic surfaces as numbered blue lines. Generalised geotechnical properties of the formations represented have been estimated from the literature (e.g. Attewell & Farmer 1976).

*Intra-formational slump at Puente Posada*

Assumed conditions post-depositional, pre-diagenesis: stability sensitive to parameter values; slope stable without a trigger when cohesion and friction higher or phreatic levels lower (after onset of diagenesis); unstable with lower cohesion and higher phreatic levels (pre-diagenetic changes).

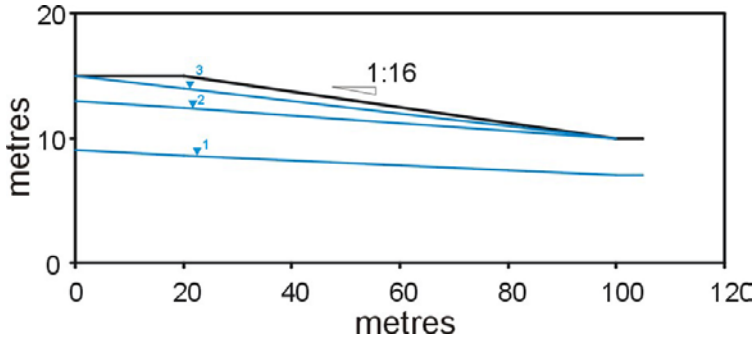


| | Bulk unit weight kN $m^{-3}$ | Unit cohesion kN $m^{-2}$ | Friction angle |
|---|---|---|---|
| Quillagua Fm. | 13 | 0 | 5 |

| | Minimum factor of safety |
|---|---|
| dry | 1.4 |
| phreatic surface 1 | 1.0 |
| phreatic surface 2 | 0.56 |
| phreatic surface 3 | 0.45 |

*Incised valley of the Río Loa at Quillagua*

Present day conditions: stable for virtually any degree of saturation.

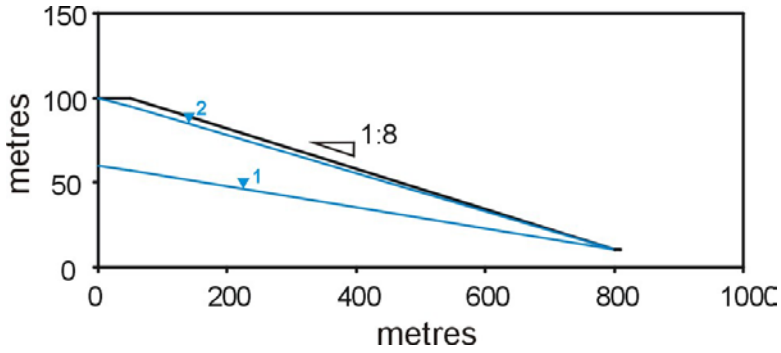


| | Bulk unit weight kN $m^{-3}$ | Unit cohesion kN $m^{-2}$ | Friction angle |
|---|---|---|---|
| Quillagua Fm. | 13 | 20 | 25 |

| | Minimum factor of safety |
|---|---|
| dry | 4.3 |
| phreatic surface 1 | 2.3 |
| phreatic surface 2 | 1.2 |

*Incised valley of the Río Loa at Yalquinche (22.45°S 68.87°W)*

Present day conditions: valley side slope stable except where water table at surface (does not occur today), thus requiring trigger for failure.

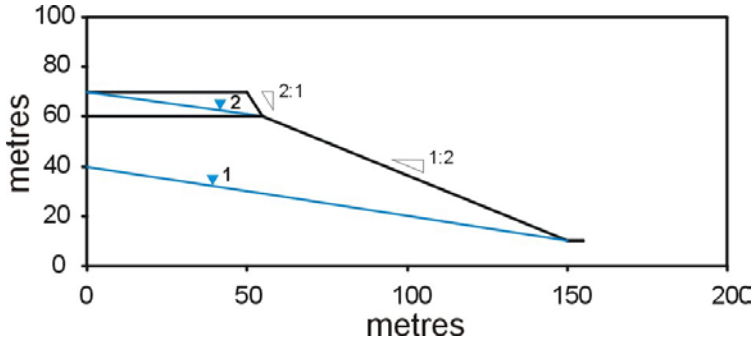


| | Bulk unit weight kN $m^{-3}$ | Unit cohesion kN $m^{-2}$ | Friction angle |
|---|---|---|---|
| Opache Formation Layer 1 | 20 | 100 | 40 |
| Jalquinche Formation Layer 2 | 18 | 20 | 30 |

| | Minimum factor of safety |
|---|---|
| dry | 1.5 |
| phreatic surface 1 | 1.3 |
| phreatic surface 2 | 1.2 |

*Sidewall erosion of the Río San Salvador at Ojos de Opache (22.47°S 69.00°W)*

Present day conditions: very stable under drained conditions even in strong earthquakes; only becomes unstable where phreatic surface at ground level (does not occur today) in strong earthquakes.

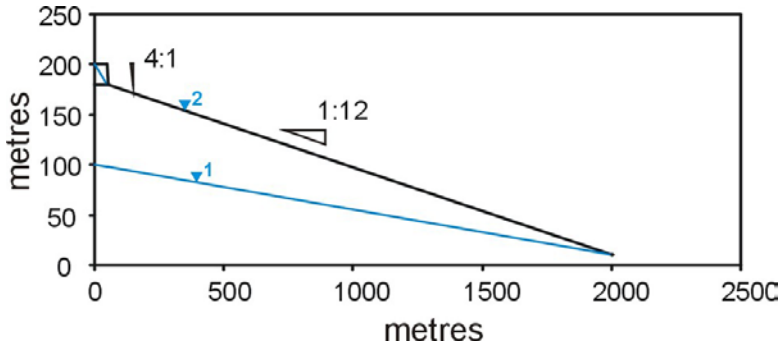


| | Bulk unit weight kN m$^{-3}$ | Unit cohesion kN m$^{-2}$ | Friction angle |
|---|---|---|---|
| Opache Formation Layer 1 | 20 | 100 | 40 |
| Jalquinche Formation Layer 2 | 18 | 20 | 30 |

| | Minimum factor of safety for given ground acceleration | | |
|---|---|---|---|
| | 0.0 | 0.2 g | 0.3 g |
| dry | 6.8 | 4.3 | 3.3 |
| phreatic surface 1 | 2.1 | 1.28 | 0.98 |
| phreatic surface 2 | 1.6 | 0.94 | 0.72 |

Attewell, P.B. & Farmer, I.W. 1976. *Principles of Engineering Geology*. Chapman and Hall, London, 1072p.

Bishop, A.W. 1955. The use of slip-circle in the stability analysis of slopes. *Geotechnique*, **1**, 125-131.

**Porosity-depth relationships in the Calama Basin**

The figure below shows combined neutron-density porosity logs averaged from three wells in the Opache (above) and Jalquinche (below) Formations, referenced to limestone and sandstone respectively. Dashed lines indicate typical values for limestones, shales and sandstones (from data in Tucker & Wright 1990; Ingebritsen *et al.* 2006). Best-fit lines are shown solid, together with the equations used subsequently in the decompaction analysis.

The inset shows grain size analyses of Jalquinche Formation samples from outcrop and wells. The sediment is bimodal with both silt and sand size peaks. These high porosity – low permeability sediments are particularly conducive to significant water retention during deposition and later slow water release (Domenico & Mifflin 1965; Meade 1968). Initial compaction, within the top few cm of the depositional surface while porosities are around 70-90%, is largely due to the mechanical rearrangement of the clay particles. Thereafter, compaction is mainly achieved through increasing

overburden pressure (Maltman 1994), although Brown & Ransom 1996 and Liu *et al*. 2006 demonstrate the role of smectite interlayer water in compaction. Jensen 1992 reports significant smectite concentrations in the Batea Formation and this is likely to be true of the Jalquinche Formation too, because most red bed sequences in the forearc are derived in part from weathering of the andesitic volcanic arc, generating smectite.

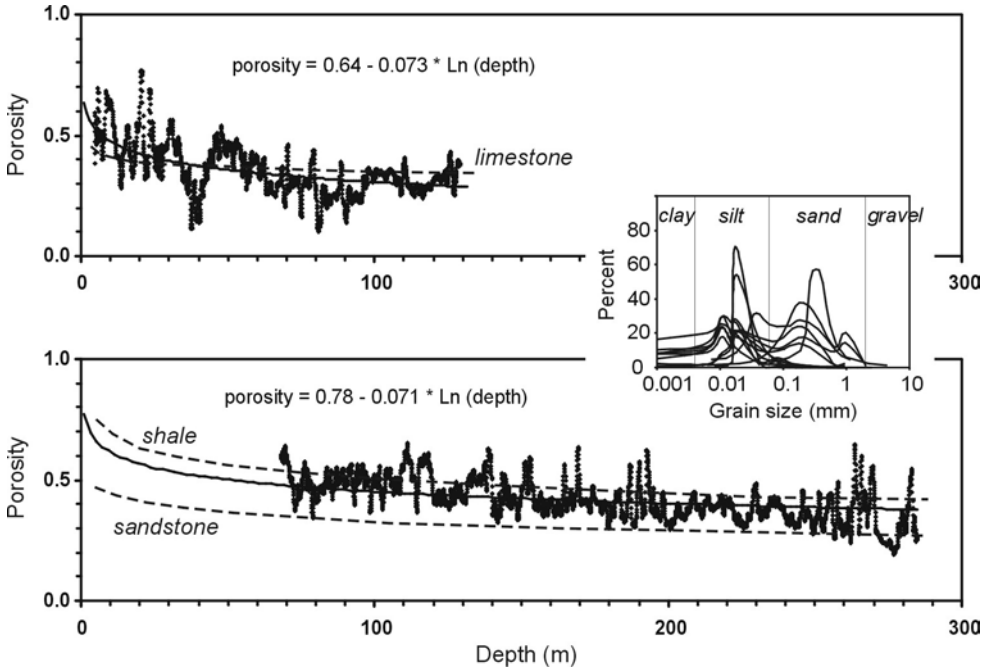


Brown, K.M. & Ransom, B. 1996. Porosity corrections for smectite-rich sediments: Impact on studies of compaction, fluid generation and tectonic history. *Geology*, **24**, 843-846.

Domenico, P.A. & Mifflin, M.D. 1965. Water from low-permeability sediments and land subsidence. *Water Resources Research*, **1**, 563-576.

Husen, S., Kissling, E., & Flueh, E.R. 2000. Local earthquake tomography of shallow subduction in north Chile: A combined onshore and offshore study. *Journal of Geophysical Research*, **105**, 183-198.

Ingebritsen, S., Sanford, W., & Neuzil, C. 2006. *Groundwater in geologic processes*. Cambridge University Press, Cambridge, 536p.

Jensen, A. 1992. *Las cuencas aluvio-lacustres Oligoceno-Neogenas de la region ante-arco de Chile Septentrional, entre los 19$^o$ y 23$^o$ Sur*. Tesis para grado, Universidad de Barcelona, 217p.

Liu, C-W., Lin, W-S. & Cheng, L-H. 2006. Estimation of land subsidence caused by loss of smectite-interlayer water in shallow aquifer systems. *Hydrogeology Journal*, **14**, 508-525.

Maltman, A.J. (ed.) 1994. *The Geological Deformation of Sediments*. Chapman and Hall, London, 362p.

Meade, R.H. 1968. *Compaction of sediments underlying areas of land subsidence in Central California*. USGS Professional Paper, No 497-D, 39p.

Tucker, M.E. & Wright, V,P. 1990. *Carbonate Sedimentology*. Blackwell, Oxford, 482p.

**Decompaction analysis of sediments in the Calama Basin**

Decompaction analysis is based on the techniques of Allen & Allen 1990 and Angevine *et al*. 1990. Sediment accumulation rates for each formation are assumed to be linear. The effects of compaction are based on the porosity-depth equations given above, and cumulated for each time step and each formation. The basement depth refers to the base of the Jalquinche Formation and not the base of the Tertiary basin infill. No corrections are made for isostasy or uplift. Calculations are given for maximum subsidence based on known thicknesses and mean subsidence based on volume (calculated from isopach maps, Nazca 2001) divided by area. Dewatering rates are based on fully saturated initial conditions with the loss in porosity at each step equivalent to the water expelled. Calculations for dewatering are necessarily based on formation volumes. The table below provides the detailed calculations.

| | | Jalquinche Fm. | Opache Fm. | Chiu Chiu Fm. |
|---|---|---|---|---|
| ages | Ma | 20-10 | 7.8-3.4 | 2.5-0.5 |
| elapsed time | Ma | 10 | 4.4 | 2.0 |
| area | $km^2$ | 2043 | 1135 | 200 |
| volume | $km^3$ | 161 | 30 | 1 |
| mean thickness | m | 79 | 26 | 5 |
| max thickness | m | 250 | 130 | 20 |
| | | | | |
| depositional porosity | | 0.78 | 0.64 | 0.70 |
| Fm. bulk porosity 0.5 Ma | | 0.46 | 0.41 | 0.60 |
| Fm. bulk porosity 3.4 Ma | | 0.47 | 0.48 | |
| Fm. bulk porosity 10 Ma | | 0.54 | | |
| column bulk porosity | | 0.54 | 0.48 | 0.46 |
| | | | | |
| matrix thickness (mean) | m | 42 | 15 | 2 |
| | | | | |
| Fm. mean thickness 0.5 Ma | m | 79 | 26 | 5 |
| Fm. mean thickness 3.4 Ma | m | 80 | 29 | |
| Fm. mean thickness 10 Ma | m | 92 | | |
| column mean thickness | m | 92 | 109 | 110 |
| column max thickness = basement depth | m | 293 | 402 | 400 |
| | | | | |
| subsidence rate mean | $m\ Ma^{-1}$ | 9.2 | 3.9 | 0.5 |
| subsidence rate max | $m\ Ma^{-1}$ | 29.3 | 24.8 | -1.0 |
| | | | | |
| porosity loss 2.5-0.5 Ma | | 0.01 | 0.07 | 0.1 |
| vol water expelled | $km^3$ | 1.8 | 2.2 | 0.1 |
| porosity loss 7.8-3.4 Ma | | 0.07 | 0.16 | |
| vol water expelled | $km^3$ | 12.6 | 7.6 | |
| porosity loss 20-10 Ma | | 0.23 | | |
| vol water expelled | $km^3$ | 85.8 | | |
| | | | | |
| total expulsion | $km^3$ | 85.8 | 20.2 | 4.1 |
| dewatering rate (mean) | $km^3\ Ma^{-1}$ | 8.6 | 4.6 | 2.1 |

Allen, P.A. & Allen, J.R. 1990. *Basin Analysis: Principles and Applications*. Blackwells, Oxford, 451p.
Angevine, C.L., Heller, P.L. & Paola, C. 1990. *Quantitative Sedimentary Basin Modelling*. AAPG Course Note Series #32, 247p.
Nazca S.A. 2001. *Pampa Llalqui Groundwater Exploration Concession: Final report to Dirección General de Aguas*. 47p.

**Estimation of subduction erosion rate**

Volcanic age dates plotted below are from Trumbull *et al*. 2006. Appendix 1 Compilation of age and location of Cenozoic volcanic centres in the Central Andes. Data are constrained by longitude (>68°W) and latitude (21°S-23°S), equivalent to the forearc and Western Cordillera of the Turi, Calama and Quillagua-Llamara Basins.

Arc retreat rates are based on the slope of a line joining westernmost volcanic centres as per method of Kukowski & Oncken 2006. Since subduction erosion is considered the principal driving force for arc retreat, the rate of arc retreat is considered equivalent to the subduction erosion rate.

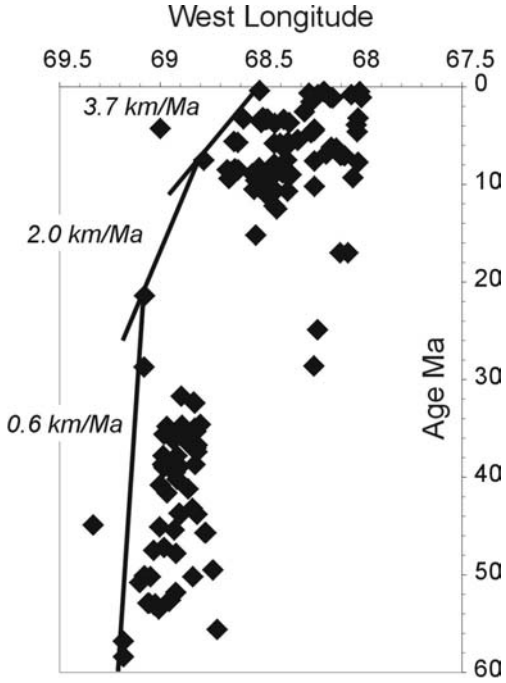


Kukowski, N. & Oncken, O. 2006. Subduction Erosion - the "Normal" Mode of Fore-Arc Material Transfer along the Chilean Margin? *In*: Oncken, O., Chong, G., Franz, G., Giese, P., Gotze, H-J., Ramos, V.A., Strecker, M.R. & Wigger, P. (eds.) *The Andes: Active Subduction Orogeny*. Springer-Verlag, Berlin, 217-136.
Trumbull, R.B., Riller, U., Oncken, O., Scheuber, E., Munier, K. & Hongn, F. 2006. The Time-Space Distribution of Cenozoic Volcanism in the South-Central Andes: A New Data Compilation. *In*: Oncken, O., Chong, G., Franz, G., Giese, P., Gotze, H-J., Ramos, V.A., Strecker, M.R. and Wigger, P. (eds.) *The Andes: Active Subduction Orogeny*. Springer-Verlag, Berlin, 29-44.

**Restoration of the Mio-Pliocene surface adjacent to the Río Loa**

The end Toconce-Opache-Quillagua Formation surface of Pliocene age (around 3Ma) can be seen as a valley-axial low-angle surface that follows the Ríos Salado and Loa westward to the Pampa Tamarugal where it turns north to the Quillagua-Llamara Basin. This surface is affected by syn- and post depositional faulting, such that it is steeper than the original depositional surface. It is possible to reconstruct the original depositional surface, assuming (1) that the coastal scarp is formed by marine erosion (Hartley and Jolley, 1995; Allmendinger et al, 2005) and not by faulting (Armijo and Thiele, 1990; Allmendinger et al, 2005) and (2) that steep slopes (>3$^{o}$ up to the east or >2$^{o}$ down to the east, based on digital 1:50,000 topographic maps) on the present day surface, represent faults and are removed on the reconstructed profile. As shown in the figure below, such steep slopes coincide with the location of major faults which are known to have been active, largely as normal faults in the Neogene, for instance the Atacama Fault Zone, the Precordillera Fault Zone, and the West Fissure system. Additional faults, which are interpreted to show evidence of Neogene movement based on this technique are the Engañada Fault, south of Quillagua, the Angostura fault, east of Calama, and the Ayquina Fault, west of Turi. The reconstructed Pliocene surface shows features that are in accord with previous studies: the Quillagua-Llamara Basin shows a down-to-the-west tilting as a result of normal displacement on the Atacama Fault (Lamb et al, 1997; Digbert et al, 2003) and down-to-the-north tilting as a result of transverse faulting (Jensen et al, 1995; Sáez et al, 1999), whilst the palaeoelevation of the Western Cordillera at ~3Ma is around 3200m (Kennan, 2000).

The reconstructed end-depositional surface of the Quillagua Formation is thus calculated as ~0.2$^{o}$; the Opache Formation as ~0.8$^{o}$ through the Precordillera, and ~0.4$^{o}$ in the Calama Basin; and the Toconce Formation as ~0.9$^{o}$.

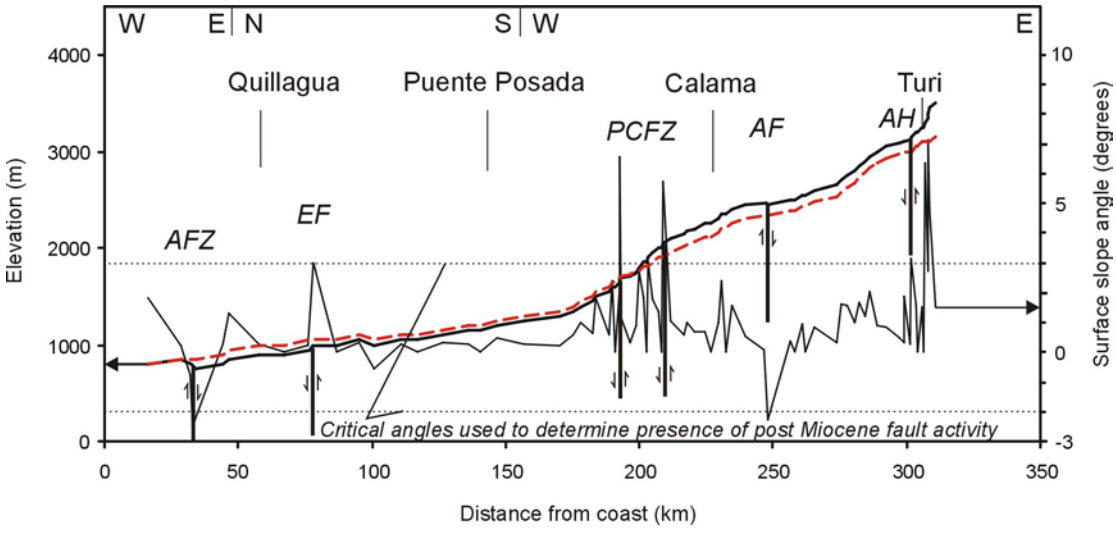


Named faults: AFZ – Atacama Fault Zone; EF - Engañada Fault; PCFZ – Precordillera Fault Zone; AF – Angostura Fault; AH – Ayquina Fault.

Allmendinger, R.W., González, G., Yu, J., Hoke, G. & Isacks, B. 2005. *Trench-parallel shortening in the northern Chilean Forearc: Tectonic and climatic implications*. Geological Society of America Bulletin, **117**, 89-104.

Armijo, R. & Thiele, R. 1990. *Active faulting in northern Chile: ramp stacking and lateral decoupling along a subduction plate boundary?* Earth and Planetary Science Letters, **98**, 40-61.

Digbert, F.E., Hoke, G.D., Jordan, T.E. & Isacks, B.L. 2003. *Subsurface Stratigraphy of the Neogene Pampa de Tamarugal basin, northern Chile*. VI Chilean Geological Congress.

Hartley, A.J. & Jolley, E.J. 1995. *Tectonic implications of Late Cenozoic sedimentation from the Coastal Cordillera of northern Chile (22-24$^{o}$S).* Journal of the Geological Society, London, **152**, 51-63.

Jensen, A., Dörr, M.J., Gotze, H.J., Kiefer, E., Ibbeken, E. & Wilke, H. 1995. Subsidence and sedimentation of a forearc-hosted, continental pull-apart basin: the Quillagua trough between 21$^{o}$30 and 21$^{o}$45 S, northern Chile. *In*: Sáez (ed.) Glopals - IAS Meeting - Chile – Abstracts, 5-6.

Kennan, L. 2000. Large-scale geomorphology of the Andes: interrelationships of tectonics, magmatism and climate. *In*: Summerfield, M.A. (ed.) *Geomorphology and Global Tectonics*. Wiley, Chichester, 167-199.

Lamb, S., Hoke, L., Kennan, L. & Dewey, J. 1997. Cenozoic evolution of the Central Andes in Bolivia and northern Chile. *In*: Burg, J.P. & Ford, M. (eds.) *Orogeny Through Time*. Geological Society, London, Special Publication No 121, 237-264.

Sáez, A., Cabrera, L., Jensen, A. & Chong, G. 1999. *Late Neogene lacustrine record and palaeogeography in the Quillagua-Llamara basin, Central Andean fore-arc (northern Chile)*. Palaeogeography, Palaeoclimatology, Palaeoecology, **151**, 5-37.